frontiers | Frontiers in Earth Science

TYPE Original Research
PUBLISHED 30 August 2023
DOI 10.3389/feart.2023.1238055

OPEN ACCESS

EDITED BY
Yi Xue,
Xi'an University of Technology, China

REVIEWED BY
Fei Guo,
China Three Gorges University, China
Defu Zhu,
Taiyuan University of Technology, China
Geng Jiabo,
Jiangxi University of Science and Technology, China

*CORRESPONDENCE
Sitao Zhu,
zhusitao@ustb.edu.cn

RECEIVED 10 June 2023
ACCEPTED 01 August 2023
PUBLISHED 30 August 2023

CITATION
Wang G, Zhu S, Zhang X, Wen Y, Zhu Z, Zhu Q, Xie L, Li J, Tan Y, Yang T, Pu Y and Zhu C (2023), Prediction of mining-induced seismicity and damage assessment of induced surface buildings in thick and hard key stratum working face: a case study of Liuhuanggou coal mine in China.
Front. Earth Sci. 11:1238055.
doi: 10.3389/feart.2023.1238055

Prediction of mining-induced seismicity and damage assessment of induced surface buildings in thick and hard key stratum working face: a case study of Liuhuanggou coal mine in China

Gaoang Wang[1], Sitao Zhu[1]*, Xiufeng Zhang[2], Yingyuan Wen[3], Zhijie Zhu[4], Quanjie Zhu[5], Liangfu Xie[3], Jiajie Li[1], Yi Tan[6], Tao Yang[4], Yuanyuan Pu[7] and Chun Zhu[7,8]

[1]School of Civil and Resource Engineering, University of Science and Technology Beijing, Beijing, China, [2]Shandong Energy Group Co., Ltd., Jinan, China, [3]College of Civil Engineering and Architecture, Xinjiang University, Urumqi, China, [4]School of Mining and Technology, Liaoning University of Engineering and Technology, Fuxin, China, [5]School of Emergency Technology and Management, North China Institute of Science and Technology, Langfang, China, [6]School of Energy Science and Engineering, Henan Polytechnic University, Jiaozuo, China, [7]State Key Laboratory of Coal Mine Disaster Dynamics and Control, Chongqing University, Chongqing, China, [8]School of Earth Sciences and Engineering, Hohai University, Nanjing, China

Thick and hard key stratum working faces are characterized by frequent mine tremors and significant ground tremors during mining which seriously threaten the safety production of the mine. With working face (4-5) 06 of Xinjiang Liuhuanggou Coal Mine as the engineering background, using field investigation, microseismic monitoring, and theoretical analysis, a mining-induced seismicity prediction method and damage assessment of surface buildings for thick and hard key stratum working faces is proposed, which is based on the evolution characteristics of overlying strata spatial structure and the motion state of the key stratum. The results of the study are as follows: 1) The movement law of overlying strata is the basis of mining-induced seismicity prediction for working faces. The magnitude of the risk of mining-induced seismicity occurrence is mainly related to the boundary conditions of the working face, the thickness of the key stratum, the distance from the coal seam to the key stratum, the height of the overlying strata spatial structure, and the fracture step of the key stratum. 2) The mining-induced seismicity energy contains the original accumulation elastic energy of the key stratum, the transfer elastic energy of low rock strata, and the accumulation elastic energy of gravity work. Based on this, a mechanical model of surface building damage induced by the release of mining-induced seismicity energy was established. A ground vibration damage boundary and vibration induction boundary under the action of strong mining-induced seismicity were proposed, and the service life of buildings when they reach the critical damage value under the action of frequent mining-induced seismicity was obtained. 3) The temporal and spatial distribution law of mining-induced seismicity activities in

thick and hard key stratum working faces was revealed. According to the results of micro-seismic monitoring, the "zonality" characteristics of the time series and the "transition" law of spatial distribution of mining-induced seismicity verified the reliability of the mining-induced seismicity prediction method. The research results provide a theoretical basis for predicting mining-induced seismicity and assessing the risk of induced disasters during the mining process of thick and hard key stratum working faces, and can provide technical support for mining-induced seismicity prevention and control and safety production in mines with similar conditions.

KEYWORDS

thick and hard key stratum, overlying strata spatial structure, prediction of mininginduced seismicity, vibration damage, the temporal and spatial distribution law

1 Introduction

Mining-induced seismicity is a dynamic phenomenon induced by mining activities and is felt within the mining area. Its essence is the violent release of elastic deformation energy of rock mass, which often induces secondary dynamic disasters (Wang et al., 2022; Jiang et al., 2013; Jiang et al., 2014; Zhu et al., 2022). There are many reasons for mining-induced seismicity in the process of underground mining. According to the different occurrence mechanisms, it can be divided into six types: movement of super-thick and hard rock strata, overall instability of coal pillars between mines, movement of surrounding rock induced by large-scale mining in mining areas, strong rockburst induced, spatial structure instability type of overlying strata induced by repeated mining, and activation of fault geological structure. The most common type is the movement of super-thick and hard rock strata. As shown in Figure 1, thick hard rock strata mining areas are widely distributed in China, such as the Yanzhou mining area in Shandong, Yima mining area in Henan, Hegang mining area in Heilongjiang, Ordos mining area in Inner Mongolia, and Liuhuanggou mining area in Xinjiang. Thick and hard rock strata accumulate high elastic properties, and high energy level mining-induced seismicity often occurs when breaking, which is very likely to induce underground dynamic disasters and damage to surface buildings.

In recent years, the frequency and energy levels of mining-induced seismicity have increased significantly in the process of coal mining, and the underground and surface safety problems induced by mining-induced seismicity have attracted more and more attention. For example, at approximately 18:00 on 7 October 2021, mining-induced seismicity occurred in the second well of the Lushan coal mine in Qitaihe City, Heilongjiang Province. The mining-induced seismicity accident caused seven miners to be trapped underground, eventually resulting in the death of three people. Mining-induced seismicity not only poses a threat to the safety of underground production but can even cause surface buildings to shake and be damaged, causing panic among personnel. A 2.4-magnitude mining-induced seismic occurred at 22:29 on 23 December 2020 in a mine in Qufu City, Jining City, Shandong Province, causing shaking in the dormitory building of Jining College, which is approximately 3 km away from the source as shown in Figure 2. A large number of students ran out of the building in their pajamas to escape, causing public concern and close attention from the government.

There are 136 mining-induced seismicity events with energy over 1 E+05J in the mining process of the (4-5) 06 fully mechanized working face along the goaf in the Liuhuanggou coal mine, of which the maximum magnitude was 3.1 (5.17 E+ 07J). Most mining-induced seismicity occurs when there is no power manifestation or slight tremor in the underground coal mine, but the floor shaking in the office building and dormitory living area in the industrial area on the ground is obvious. The frequency and intensity of mining-induced seismicity in the working face are much higher than that of the 1,000-km underground roadway in eastern China, which has significant safety risks. It is of great practical significance to study the occurrence law of mining-induced seismicity and the assessment of the vibration damage of mining-induced seismicity to the facilities near the ground. The research results can provide a reliable basis for the prevention and control of major hazards.

A large number of research studies have been conducted around the topic of mining-induced seismicity, mainly focusing on mining-induced seismicity mechanism and type classification (Jan et al., 2018; Liu et al., 2020; Lurka, 2021; Dou et al., 2021; Zhu et al., 2022), mining-induced seismicity induced hazard types and prediction (Grzegorz et al., 2020; Ma et al., 2018; RUSEK, 2017), mining-induced seismicity induced underground rock burst (Lu et al., 2021; Liu et al., 2021), gas outburst (Xue et al., 2023; Ye et al., 2023), water invasion (Zhang et al., 2023; Hou et al., 2023), and surface building vibration damage prevention and control (Zhu et al., 2021; Xue et al., 2023).

Wang et al. (2019) analyzed the mining-induced seismicity activity patterns in different mining stages of coal mines based on the distribution characteristics of microseismic events and obtained the types of surrounding rock damage as tensile damage and shear damage. Baranov et al. (2021) studied the characteristics of the spatial distribution of mining-induced seismicity events induced by geotectonic activation under mining conditions and developed a model of the maximum distance from the source of mining-induced seismicity to the predicted induced aftershock. Chlebowski et al. (2021) investigated the qualitative and quantitative indicators characterizing the seismic activity of rock formations, established a stress state analysis model to predict mining-induced seismicity levels, and verified the correlation between changes in mining-induced seismicity activity and model tests. Sokoła-Szewioła et al. (2019) studied the use of a GIS classification system to predict and evaluate the effects of mining-induced seismicity on surface buildings, the results of which showed that numerous information on mining-induced

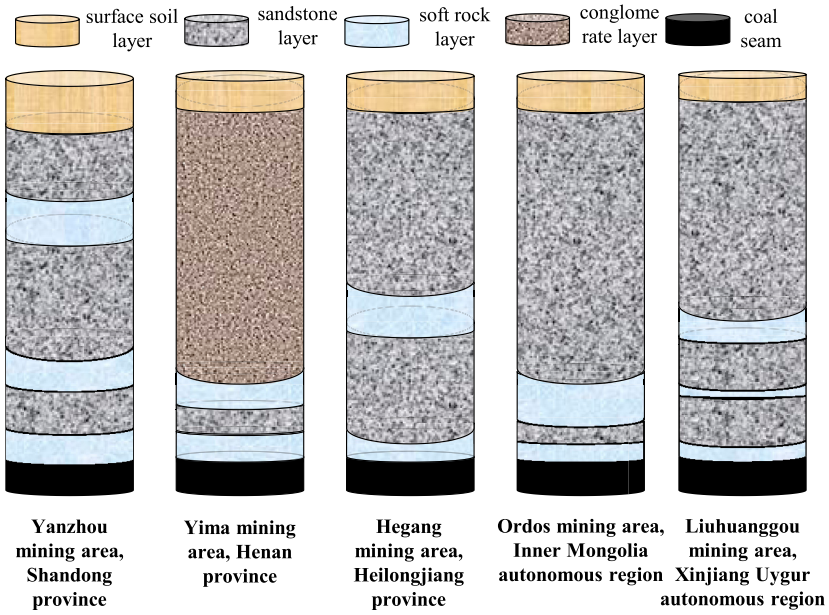

FIGURE 1
Distribution of thick and hard rock strata in main coal mine areas in China.

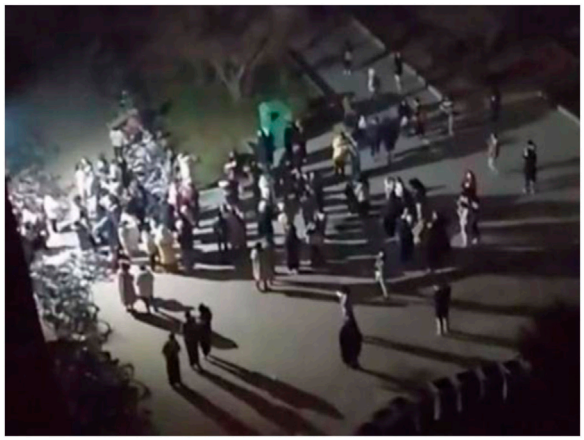

FIGURE 2
Screenshot of the video of students fleeing the scene during the mining-induced seismicity.

seismicity-induced ground vibrations, including object damage, can be recorded using the ArcGIS system. Guangyao et al. (2020) established a probability density function containing spatial, temporal, and energy parameters of mining-induced seismicity activity and proposed the probability density distribution values as an indicator of the degree of mining-induced seismicity event clustering and used them to predict the location of high energy level mining-induced seismicity events. Ryszard et al. (2020) investigated the surface deformation caused by mining-induced seismicity activity using satellite radar interferometry, and the results showed that the surface subsidence caused by mining-induced seismicity is usually in a regular elliptical shape, and the surface will be deformed when the energy of mining-induced seismicity exceeds 1E+05J magnitude. Yang et al. (2019) proposed the use of directional hydraulic fracturing of the hard roof to reduce the mining-induced seismicity load, which ensured the safe recovery of the working face. Liu (2021) used the measures of pre-fracture blasting of the roof, large diameter drilling of the coal seam, and blasting of the coal seam to unload pressure to effectively reduce the risk of mining-induced seismicity induced rockburst. Studies have been conducted to play an important role in understanding the underground rockburst and surface building hazards induced by mining-induced seismicity, but fewer studies have been conducted to quantitatively predict the relationship between the state of key stratum movement and the damage of surface buildings during coal mining. Moreover, research has only conducted small-scale fracturing and blasting on low-level roofs underground, resulting in poor effectiveness in preventing and controlling mining-induced disasters in high-level rock formations. This has failed to achieve the source prevention and control of mining-induced seismicity induced disasters in coal mines.

Although mining-induced seismicity and rockburst are both dynamic phenomena in coal mining, mining-induced seismicity is different from rockburst. Rockburst is mainly caused by the sudden release of energy caused by stress concentration, which causes roadway damage and casualties (Yin et al., 2021; Ren et al., 2023). Measures such as actively reducing stress concentration and improving roadway support capacity are often taken to prevent it (Wang et al., 2022; Li et al., 2023; Jiang et al., 2023), which makes rockburst an avoidable dynamic disaster. Mining-induced seismicity is an inevitable dynamic phenomenon in the process of coal mining. Energy release induces underground mining space rockburst and surface building damage, that is, mining-induced seismicity can induce rockburst. Therefore, it is particularly important to predict the intensity and evaluate the

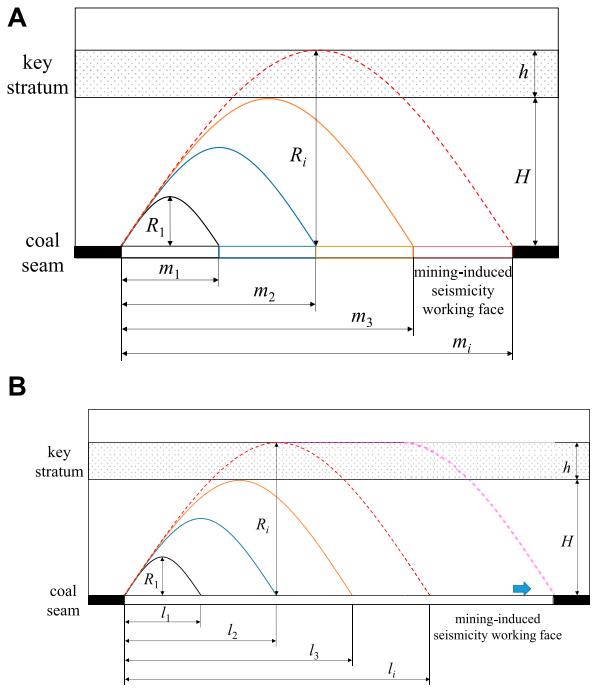

FIGURE 3
Schematic diagram of spatial structure evolution characteristics of overlying strata in a thick and hard key stratum working face. **(A)** Spatial structure evolution characteristics of inclined overlying strata in the continuous working face. **(B)** Spatial structure evolution characteristics of overlying strata in strike mining of mining-induced seismicity working face.

degree of damage from mining-induced seismicity induced dynamic disasters. The grade of the overlying strata movement type of mining-induced seismicity is related to the movement state of the key stratum. The maximum energy mining-induced seismicity occurs during the initial fracture of the key stratum, and the frequency of the key stratum rotation and slip type of mining-induced seismicity is high but the energy is low. Therefore, this article mainly focuses on the initial fracture-type mining-induced seismicity in the key stratum with high energy levels and high damage and solves the problems of "when and where the mining-induced seismicity will occur when the working face is mined," "what is the maximum energy level of the mining-induced seismicity" and "the intensity of the maximum level of the mining-induced seismicity." Based on this, firstly, the evolution law of spatial structure of overlying strata in thick and hard key stratum working faces is studied, and an ultimate fracture mechanics model of the thick and hard key stratum based on the thick plate theory is established. Furthermore, a fracture-type mining-induced seismicity prediction method of the thick and hard key stratum based on the evolution law of spatial structure of overlying strata and the movement state of the key stratum is proposed. Secondly, the released energy of key stratum fracture-type mining-induced seismicity is estimated, and the assessment criterion of surface building damage induced by high energy level mining-induced seismicity based on particle vibration velocity and the service life criterion of buildings under frequent low energy level mining-induced seismicity are given. Finally, the spatial structure evolution characteristics of overlying strata during the whole process of mining in thick and hard key stratum are studied, and the reliability of mining-induced seismicity prediction guidelines and disaster hazard assessment guidelines are verified by the time-space distribution law of mining-induced seismicity. This article proposes a mining-induced seismicity prediction method and hazard assessment method based on the spatial structure evolution characteristics of overlying strata and the motion state of key stratum in the working face. It can quantitatively calculate the magnitude of mining-induced seismicity energy through different mining stages, and achieve quantitative prediction of mining-induced seismicity and hazard throughout the whole mining cycle of the working face and mine. The research results are of great significance for mining-induced seismicity prevention and safety production guarantees during the mining process of thick and hard key stratum in mines.

2 Research on mining-induced seismicity prediction method for thick and hard key stratum working faces based on overlying strata movement

2.1 Evolution characteristics of overlying strata spatial structure in a thick and hard key stratum working face

After the coal seam is mined, the overlying strata fracture forms an overlying strata spatial structure. With the continuous advancement of the working face, the spatial structure range of the overlying strata and the movement state of the strata will dynamically evolve, and the fracture movement of the key stratum will induce mining-induced seismicity. Therefore, the study of the movement law of the overlying strata is the basis for the prediction of the mining-induced seismicity in the working face. The dynamic evolution model of overlying strata spatial structure in the continuous mining process of thick and hard key stratum is shown in Figure 3. In the figure, m is the width of the working face, H is the distance from the coal seam to the key stratum, h is the thickness of the key stratum, l is the advancing distance of the working face, and R is the height of the overlying strata spatial structure of the working face.

According to the academic viewpoint of overlying strata spatial structure, the fracture height of overlying strata is closely related to the width of the goaf. Before the stratum enters the critical mining state, the "square position" makes the fractured rock stratum reach the highest value in stages, and the fracture height of the overlying strata in the stope is approximately half of the short side length of the goaf (Jiang et al., 2003). As shown in Figure 3A, for the continuous mining face, the change in the boundary conditions of the stope leads to a significant change in the fracture morphology of the rock strata in space, and the height of the overlying strata spatial structure is constantly increasing. Due to the high strength of the thick and hard key stratum, there is a nonlinear relationship between the fracture height of the overlying strata in the vertical direction and the width of the goaf, namely, the "platform effect" (Zhang et al., 2018). However, there must be a key working face that makes the rock stratum fracture height exceed the height of the key stratum

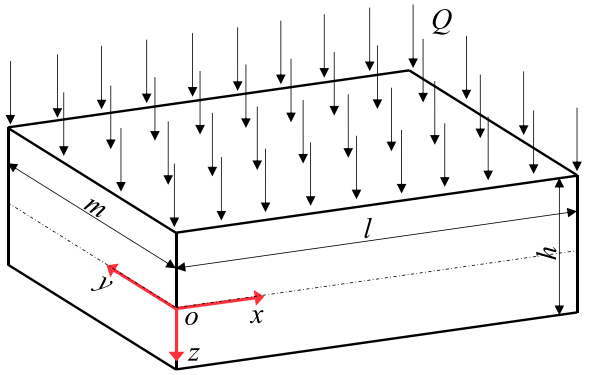

FIGURE 4
Simplified thick plate mechanical model of key stratum.

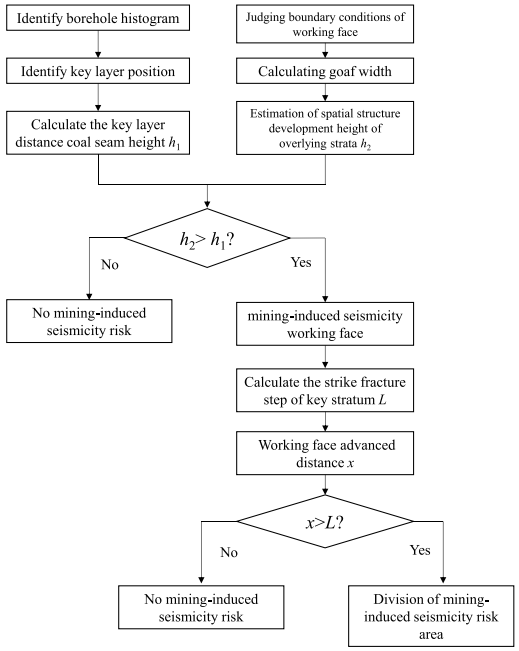

FIGURE 5
Prediction flow chart of mining-induced seismicity possibility in the thick and hard key stratum.

from the coal seam, which is called the " mining-induced seismicity working face" in this article. From the perspective of disaster prevention and control, the "mining-induced seismicity working face" is the working face where the main key stratum is broken, causing a change in danger. It is also the key area for the prevention and control research and mining optimization of the mining range. As shown in Figure 3B, when the "mining-induced seismicity working face" is mined, the thick and hard key stratum begins to suspend under the action of the multiple square positions of the working face. When the advancing distance of the working face exceeds the fracture step of the key stratum, the motion state of the key stratum changes, and the key stratum breaks under tension and releases the high elastic performance accumulated by itself to induce mining-induced seismicity.

2.2 Fracture mechanics model of a thick and hard key stratum

With the mining of the mining-induced seismicity working face, the overhanging area of the key stratum increases, causing damage at the fracture boundary of the goaf. The boundary around the key stratum moves to a plastic hinged state, and the boundary conditions change from four edges clamped support to four edges simple support. However, at this time, the key stratum as a whole is not damaged, but the boundary constraint is weakened. When it is affected by mining, fracture instability will occur. Accordingly, the key stratum is simplified as four edged simply supported rectangular thick plate subjected to uniform load, as shown in Figure 4. The Cartesian coordinate system is established with the intersection point of the neutral surface of the key stratum as the origin o. The x direction is the advancing direction of the working face, the y direction is the inclined direction of the goaf, and the z direction is the height direction. In the figure, Q is the self-weight stress of the overlying strata of the key stratum (including its own thickness), l is the overhanging length of the key stratum in the advancing direction of the working face, m is the overhanging width in the inclined direction of the goaf, and h is the thickness of the key stratum.

According to Vlasov's thick plate theory (Zuo et al., 2021), the bending moment equation of the four edges simply supported thick plate is

$$\begin{cases} M_x = \dfrac{D}{5}\left[\dfrac{Q\left(\frac{5}{l^2}+\frac{4\mu}{lm}+\frac{\mu}{m^2}\right)}{D\pi^2\left(\frac{1}{l^2}+\frac{1}{m^2}\right)^2}+\dfrac{6Q\mu\left(\frac{1}{m^2}-\frac{1}{lm}\right)}{5Gh\left(\frac{1}{l^2}+\frac{1}{m^2}\right)}\right]\times sin\,\dfrac{\pi x}{l}\,sin\,\dfrac{\pi y}{m} \\ M_y = \dfrac{D}{5}\left[\dfrac{Q\left(\frac{5}{l^2}+\frac{4\mu}{lm}+\frac{\mu}{m^2}\right)}{D\pi^2\left(\frac{1}{l^2}+\frac{1}{m^2}\right)^2}+\dfrac{6Q\mu\left(\frac{1}{l^2}-\frac{1}{lm}\right)}{5Gh\left(\frac{1}{l^2}+\frac{1}{m^2}\right)}\right]\times sin\,\dfrac{\pi x}{l}\,sin\,\dfrac{\pi y}{m} \end{cases} \tag{1}$$

From Eq. 1, we know that M_x has a maximum value at $x = l/2$, M_y has a maximum value at $y = m/2$, and $M_{x\max} = M_{y\max}$. Thus, we can make $M_{\max} = M_{x\max}$, that is

$$M_{\max} = M_{x\max} = \frac{D}{5}\left[\frac{Q\left(\frac{5}{l^2}+\frac{4\mu}{lm}+\frac{\mu}{m^2}\right)}{D\pi^2\left(\frac{1}{l^2}+\frac{1}{m^2}\right)^2}+\frac{6Q\mu\left(\frac{1}{m^2}-\frac{1}{lm}\right)}{5Gh\left(\frac{1}{l^2}+\frac{1}{m^2}\right)}\right] \tag{2}$$

The tensile stress on the lower surface of the thick plate is the maximum value, then

$$\begin{aligned} \sigma_{\max} &= \frac{12M_{\max}}{h^3}\times z = \frac{12M_{\max}}{h^3}\times\frac{h}{2} = \frac{6M_{\max}}{h^2} \\ &= \frac{6Q\left(\frac{5}{l^2}+\frac{4\mu}{lm}+\frac{\mu}{m^2}\right)}{5\pi^2\left(\frac{1}{l^2}+\frac{1}{m^2}\right)^2h^2}+\frac{6Q\mu\left(\frac{1}{m^2}-\frac{1}{lm}\right)}{25\left(1-\mu\right)\left(\frac{1}{l^2}+\frac{1}{m^2}\right)} \end{aligned} \tag{3}$$

The mechanical criterion for the fracture of the key stratum is that the fracture occurs when the maximum tensile stress $\sigma_{\max}$ reaches its ultimate tensile strength σ_t, that is,

$$\sigma_{max} = \sigma_t = \frac{6Q\left(\frac{5}{l^2} + \frac{4\mu}{lm} + \frac{\mu}{m^2}\right)}{5\pi^2\left(\frac{1}{l^2} + \frac{1}{m^2}\right)^2 h^2} \frac{6Q\mu\left(\frac{1}{m^2} - \frac{1}{lm}\right)}{25(1-\mu)\left(\frac{1}{l^2} + \frac{1}{m^2}\right)} \quad (4)$$

Let $\frac{6Q}{5\pi^2h^2} = \lambda_1$, $\frac{6Q\mu}{25(1-\mu)} = \lambda_2$, $\frac{1}{l} = a$, then Eq. 4 can be changed into

$$\sigma_t a^4 + \frac{\lambda_2}{m}a^3 + \left(\frac{2\sigma_t - \lambda_2}{m^2} - 5\lambda_1\right)a^2 + \left(\frac{\lambda_2}{m^3} - \frac{4\lambda_1\mu}{m}\right)a + \left(\frac{\sigma_t - \lambda_2}{m^4} - \frac{\lambda_1\mu}{m^2}\right) = 0 \quad (5)$$

Thus, the unary quartic equation of the inverse function of the fracture step of the key stratum based on the thick plate theory can be obtained, and the analytical solution of the fracture step of the key stratum can be obtained by Eq. 5.

2.3 Method for predicting the possibility of mining-induced seismicity occurrence in thick and hard key stratum working face

According to the evolution characteristics of the overlying strata spatial structure of the thick and hard key stratum, the main influencing factors for the occurrence of fracture-type mining-induced seismicity in the thick and hard key stratum are as follows: the boundary conditions of the working face (width of goaf), the distance from the coal seam to the key stratum, the height of the overlying strata spatial structure, the thickness of the key stratum, the fracture step of the key stratum, and the advancing length of the working face.

Based on the principle of the universal applicability of the prediction method, this article mainly studies the evolution characteristics of the overlying strata spatial structure and the fracture step of the key stratum in thick and hard key stratum stopes under typical mining boundary conditions, without considering the influence of special geological conditions and mining conditions. According to this, the flow of the prediction method for the possibility of mining-induced seismicity in the thick and hard key stratum can be obtained as shown in Figure 5.

In the first step, the thickness variation of the key stratum is obtained according to the mine strata histogram and then the height of the key stratum is determined. Finally, the height h_1 of the key stratum from the coal seam is determined.

In the second step, according to the mining situation of the adjacent area of the pre-mining face, the boundary conditions of different stages of the stope mining process are divided, and the development height h_2 of the spatial structure of the overlying strata is estimated.

In the third step, a numerical comparison is made between the height h_1 of the key stratum from the coal seam with the height h_2 of the overlying strata spatial structure. If $h_1 > h_2$, there is no risk of mining-induced seismicity in the working face. If $h_2 > h_1$, the pre-mining working face is defined as " mining-induced seismicity."

In the fourth step, based on the thick plate theory and the mechanical parameters of the key stratum, the fracture step L of the thick and hard key stratum is calculated. When the advancing distance x of the working face exceeds the fracture step L of the thick and hard key stratum, the working face is at risk of mining-induced seismicity, and the working face mine seismic hazard zone is defined accordingly.

3 Assessment of damage of surface buildings induced by mining-induced seismicity in a thick and hard key stratum working face

The essence of key stratum fracture-type mining-induced seismicity is that the high elastic energy released by the fracture of the thick and hard rock stratum is transformed into kinetic energy and transmitted to the surrounding area in the form of a vibration wave to form a vibration phenomenon. Since a high-located key stratum is close to the surface, high energy level mining-induced seismicity generated by the fracture of a high-located key stratum will pose a great threat to the surface buildings. Within the mining area of the Liuhuanggou coal mine, there are industrial square office areas and staff living areas on the ground. In total, 136 mining-induced seismic events with energy levels above 1E+05J occurred during the mining period at the (4-5) 06 working face, which caused frequent shaking of the office and dormitory buildings on the ground, causing great psychological panic to the staff and living personnel in the mine. Therefore, it is necessary to evaluate the induced disaster of mining-induced seismicity caused by working face mining to ensure the safety and stability of surface buildings during working face mining.

3.1 Estimation of mining-induced seismic energy induced by the fracture of a thick and hard key stratum

The fracture-type mining-induced seismic energy U of the key stratum mainly comes from three parts. The first is the elastic energy U_1 which accumulates in the high-located key stratum under the action of the overlying rock layer and its own large thickness self-weight stress, the second is the elastic energy U_2 which accumulates under the action of the horizontal stress transferred by the breakage of the low-located key stratum, and the third is the elastic energy U_3 which is generated by the work of the instantaneous settlement movement after the breakage of the high-located key stratum flexural deformation. Therefore, the elastic energy released during the fracture and settlement of the key stratum can be expressed as.

$$U = U_1 + U_2 + U_3 \quad (6)$$

Assuming that the key stratum is a homogeneous elastomer, the work done by the overlying strata and its own self-weight stress will all be stored in the key stratum in the form of elastic energy, then the accumulation of original elastic energy in the key stratum is.

$$U_1 = \iiint_V U_V dV = \iiint_V \frac{(1-2\mu)(1+\mu)^2}{6E(1-\mu)^2}\gamma^2H^2dV = \frac{(1-2\mu)(1+\mu)^2}{6E(1-\mu)^2}\gamma^2H^2lmhI \quad (7)$$

In the formula, E is the elastic modulus of the key stratum, γ is the average bulk density of the key stratum and the overlying strata, and H is the height from the ground surface to the lower surface of the key stratum.

When the rock stratum breaks, its accumulated elastic energy will be transferred to the upper and lower hard rock strata respectively. Since all the lower layers of the high-located key

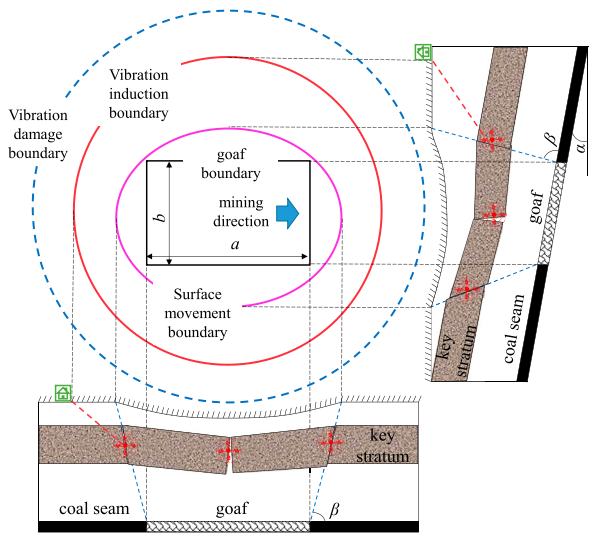

FIGURE 6
Mechanical model of vibration damage induced by fracture-type mining-induced seismicity in thick and hard key stratum working face.

stratum have been broken, it can be assumed that all the residual elastic energy of the fracture of the lower stratum is transferred to the key stratum:

$$U_2 = \zeta \frac{(1-2\mu_i)(1+\mu_i)^2}{6E_i(1-\mu_i)^2} \gamma^2 H_i^2 l_i m_i h_i \tag{8}$$

In the formula, ζ is the elastic energy transfer coefficient of the low rock strata, $0<\zeta<1$.

The key stratum will undergo flexural deformation before breaking, and when it breaks, it will produce an instantaneous settlement.

During the settlement process, the broken rock blocks work under the action of gravity to form gravitational potential energy, and its value is linearly proportional to the height of free settlement space h_0, that is,

$$U_3 = mgh_0 = \rho Vgh_0 = \rho lmhgh_0 \tag{9}$$

Substituting Eqs 7–9 into Eq. 6, the elastic energy U released in the process of fracture settlement of key stratum can be obtained as

$$U = \frac{(1-2\mu)(1+\mu)^2}{6E(1-\mu)^2} \gamma^2 H^2 lmh + \zeta \frac{(1-2\mu_i)(1+\mu_i)^2}{6E_i(1-\mu_i)^2} \gamma^2 H_i^2 l_i m_i h_i + \rho lmhgh_0 \tag{10}$$

Since the elastic energy calculated in Eq. 10 is based on the homogeneous elasticity of the key stratum, this is without considering the dissipated energy of plastic deformation of the key stratum and other forms of energy dissipated in the process of elastic energy release. In fact, the key stratum fracture release energy U is converted into kinetic energy transfer in the form of vibration waves U_K as

$$U_K = KU, \tag{11}$$

In the formula, K is the conversion rate of breaking release energy into vibration energy, and its value is 1%–5%.

3.2 Analysis of ground vibration damage effects induced by mining-induced seismicity

Figure 6 shows the mechanical model of surface building damage induced by key stratum fracture-type mining-induced seismicity. Therefore, the damage assessment criterion of key stratum fracture-type mining-induced seismicity based on "goaf boundary—surface movement boundary—vibration damage boundary" can be obtained.

The experimental study shows that when the energy released from the rock fracture is transmitted in the form of vibration waves, due to the heterogeneity of the stratum structure, the energy decays according to the multiplicative power relationship when it reaches the surface, that is, the energy reaching the surface is inversely related to the spatial distance of the seismic source, and the decayed energy is (Zhu et al., 2022).

$$U_R = \lambda U_K R^{-\eta} \tag{12}$$

In the formula, λ is the energy conversion efficiency between vibration energy and particle kinetic energy; η is the attenuation coefficient of vibration wave, whose value is related to stratum structure.

When the energy U_R transmitted to the ground building after the mining-induced seismicity energy has been attenuated by the strata exceeds the critical damage energy U_m of the building, damage to the building occurs, that is, when.

$$U_R > U_m \tag{13}$$

3.3 Guidelines for assessing surface building damage induced by mining-induced seismicity

The types of mining-induced seismicity induced by overlying strata fracture during coal mining can be divided into two categories, one is the initial fracture of the high-located key stratum inducing high energy level mining-induced seismicity, and the other is the periodic fracture of the high-located key stratum and low-located key stratum fracture inducing low energy level mining-induced seismicity. Under the action of different energy levels of mining-induced seismicity, the damage types of surface buildings can also be divided into two types. One is the direct damage of the buildings under the action of high energy level mining-induced seismicity, and the other is the gradual reduction of the bearing performance of the buildings under the frequent action of low energy level mining earthquakes, which eventually leads to the destruction of buildings.

3.3.1 Assessment method for vibration damage of surface buildings induced by high energy level mining-induced seismicity

The particle vibration velocity v_m is generally used as the building vibration damage standard (Wu et al., 1997) According to its value, the critical energy required for surface building damage to occur can be derived. The critical energy per unit volume of particle vibration damage is.

$$U_m = \frac{1}{2}\rho v_m^2 \tag{14}$$

Substituting Eqs 12, 14 into Eq. 13, we can get the discriminative condition for the surface building vibration damage induced by the key stratum fracture-type mining-induced seismicity energy waves as.

$$R = \left(\frac{2\lambda U_K}{\rho v_m^2}\right)^{\frac{1}{\eta}} \tag{15}$$

The magnitude of mining-induced seismicity intensity is not only related to the energy level of mining-induced seismicity but is most importantly limited by the distance between the seismic source and the building. Generally, the main key stratum is buried shallowly and the vertical distance between it and the ground is small, so the vibration propagation distance can be simplified to the plane distance between the seismic source and the building. The extent of the impact of high-located key stratum fracture-type mining-induced seismicity is divided into 2 boundaries based on the degree of damage to surface buildings and the degree of personnel perception by vibration wave transmission: 1) Vibration damage boundary R_1, particle vibration velocity v_m = 30 mm/s, the surface buildings within this boundary are damaged and may cause casualties; and 2) vibration induction boundary R_2, particle vibration velocity v_m = 5 mm/s, within this boundary the surface buildings will not be damaged, but people will feel the tremors clearly and panic will arise psychologically. Beyond the latter boundary, the surface buildings will not be damaged, and the tremors are not obvious to the personnel.

3.3.2 Vibration damage assessment method for surface buildings induced by frequent low energy level mining-induced seismicity

Field practice shows that when low energy level mining-induced seismicity occurs, no damage occurs to the buildings on the ground, but the long-term effects of the mining-induced seismicity will produce damage to the building structure and reduce the safe service life of the building. The damage value of the building can be solved by the degree of change in the natural frequency of the building structure, that is, the damage value d_i of the ith component in the building is (Wang et al., 2021).

$$d_i = 1 - \frac{f_i^2}{f_0^2} \tag{16}$$

In the formula, f_0 is the natural frequency of the component without damage; f_i is the natural frequency of the component after damage.

The damage value D of the overall structure of the building can be obtained from the weighted combination of the damage values of each grouped member. The natural frequency change of the building structure can be obtained through vibration testing, and then the overall damage value D can be obtained. It has been shown that the service life of a building under the effect of the frequent mine earthquakes of mining-induced seismicity when it reaches a critical damage value can be expressed as.

$$T = \frac{N}{f \times t \times n} \tag{17}$$

In the formula, N is the number of building fatigue damage vibrations, f is the average vibration frequency of mining-induced seismicity, t is the average wave delay time, and n is the average number of mining-induced seismicity per year.

4 Engineering applications

4.1 Project overview

Liuhuanggou Coal Mine (4-5) 06 comprehensive caving working face is adjacent to the (4-5) 04 mining area and the (4-5) 02 mining area. The designed strike length is 1726.5 m and the inclination length is 183 m. The working face is mining a 4-5 coal seam. The coal seam inclination angle is 25°~33°, average 29°, the coal seam thickness is 6.24~6.92 m, and the average thickness is 6.52 m. The working face elevation is +777.5~+716.3 m, and the surface elevation is +1,135.5~+1,242.5 m. The (4-5) 06 working face open cut is outside the (4-5) 02 working face open cut by approximately 650 m, as shown in Figure 7 According to the coal-rock rockburst tendency identification, the 4-5 coal seam, the roof strata, and the floor strata all have a weak rockburst tendency, among which the single axis compressive strength of the 4-5 coal seam is 13.34 MPa. The structural characteristics of the roof strata of the 4-5 coal seam obtained from the column diagram of hole 27-2 of the mine are shown in Figure 7. The roof strata of the 4-5 coal seam is dominated by siltstone, with a total of five sandstone groups from the main roof to the surface, with mudstone of varying thickness distributed between the layers. A microseismic monitoring method records the energy released by the coal and rock mass fracture and vibration induced during the mining process to analyze and determine the direction of vibration propagation, accurately locate the source location, and calculate the energy. The mine has installed the ARAMIS M/E microseismic monitoring system, and at least 4 microseismic detectors have been installed while mining the (4-5) 06 working face, which can monitor the rockburst hazard areas of different levels. The ARAMIS M/E microseismic monitoring system integrates a digital DTSS transmission system, collecting data for mine vibration positioning, vibration energy calculation, and vibration hazard assessment. Sensors (sensors or other) monitor vibration events and process them into digital signals, which are then transmitted to the ground by the digital signal transmission system DTSS. The system can monitor vibration events with a vibration capacity greater than 100J, a frequency range of 0~150 Hz, and less than 110 dB (anti-interference ability). According to the different monitoring ranges, the system can choose sensors with different frequency ranges. The data transmission system allows for the transmission of three-dimensional vibration rate change (X, Y, Z) signals through a long-distance transmission cable. The system provides the conversion and recording of vibration signals through a 24-bit σ-δ converter, and completes continuous and real-time vibration monitoring based on the recording server. The standard version of the system software provides one monitoring signal for each channel; The optional 3-channel signal monitoring for each channel requires non-standard software that can monitor microseismic activity in three directions.

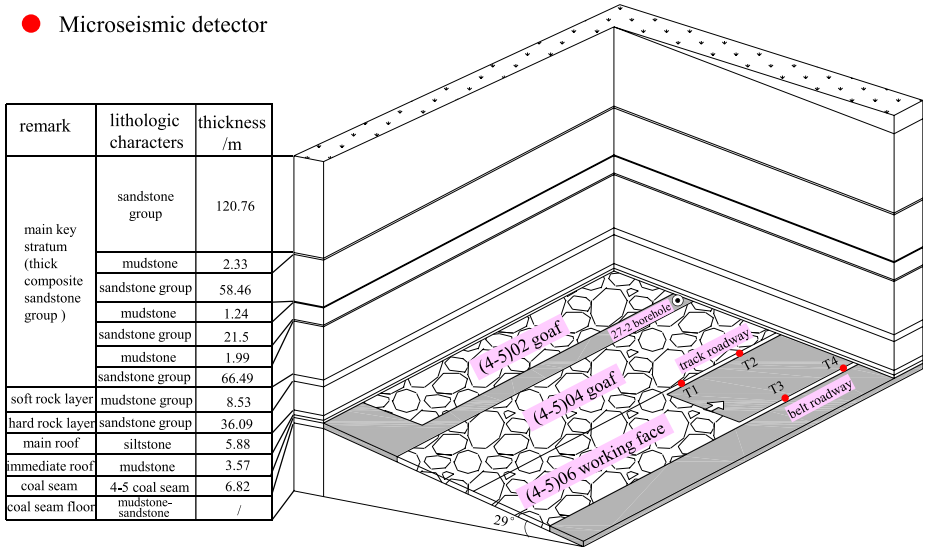

FIGURE 7
Schematic diagram of fully mechanized mining face along gob in inclined thick coal seam.

TABLE 1 Key stratum movement state.

Working face name	Surface subsidence/m	Coefficient of sinking	Whether fully adopted	Key stratum state
(4–5) 02	3.312	0.51	no	overhanging top
(4–5) 04	1.721	0.27	no	overhanging top
(4–5) 06	1.627	0.25	no	overhanging top

According to the observation data of surface subsidence in the Liuhuanggou coal mine on 6 November 2019, before the (4-5) 06 working face was mining to the square of three working faces, the value of surface subsidence is small, all of them were in non-sufficient mining states. From this, it can be judged that the key stratum still maintained its own complete stability and was in a state of hanging roof (Table 1).

Based on the structural characteristics of the column diagram of hole 27-2 of the mine, the spatial and temporal distribution pattern of mine seismic events during the mining of the (4-5) 06 working face and the surface subsidence data, the key stratum of the working face is divided as shown in Figure 7. The inferior key stratum is the sandstone group with a thickness of 36.09 m at 9.45 m from the coal seam, and the main key stratum is the thick composite sandstone group with a thickness of 272.77 m at 54.07 m from the coal seam.

4.2 Analysis of the law of spatial structure evolution of overlying strata in working face

During the mining period, the (4-5) 06 working face will encounter the partition of mining conditions. Based on the changes in the boundary conditions of the working face in different mining stages, the dynamic evolution model of overlying strata spatial structure of the (4-5) 06 working face during the whole mining process is established in this article as shown in Figure 8. As shown in Figure 8A, the mining process of the working face is divided into five movement stages, depending on changes in the overlaying strata's spatial structure planform and spatial height. These are as follows.

(1) Low-located roof strata movement stage.

The mining range corresponds to the distance between the working face from the position of the open-off cut to the square position of the single working face. The characteristics of rock movement are characterized by a small-scale fracture of the low-located roof strata of the working face. The spatial structure of the overlying strata formed when the working face is mined from the open-off cut is shown in Figure 8B. With the working face mining, the range of fractured overburden strata in the working face increases along the mining direction and rises gradually along the height direction. When the working face is mined to the square position of the single working face, the fracture height of the overburden strata reaches the same layer as the fractured overburden strata in the (4-5) 04 goaf, as shown in Figure 8C. During this stage, the energy released from the fracture of the low-located roof strata is small, so the energy of mining-induced seismicity is low and the frequency is low, and it is in the quiet period of mining-induced seismicity.

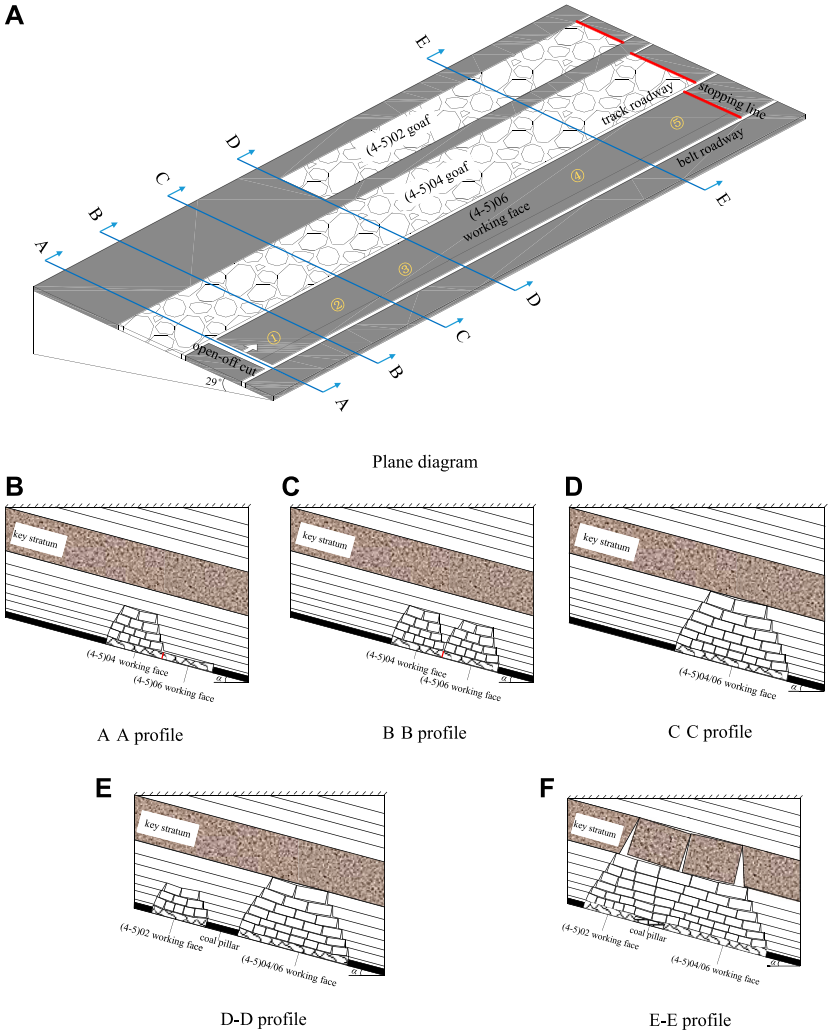

FIGURE 8
Schematic diagram of the dynamic evolution of the overlying strata spatial structure during the whole process of mining in (4-5) 06 working face. **(A)** Plane diagram **(B)** A-A profile **(C)** B-B profile **(D)** C-C profile **(E)** D-D profile **(F)** E-E profile.

(2) Overlying strata spatial structure expansion stage.

The mining range corresponds to the distance between the working face from the position of the single working face to the flush position of the original (4-5) 02 open-off cut. The characteristics of rock movement are characterized by a series of movements of the overlying strata in the goaf and the formation of a small structure of overlying strata in two goaves. With the mining of the working face, periodic fractures occur in the roof strata. Because of the small coal pillar arrangement between the (4-5) 06 working face and the (4-5) 04 working face, the roof strata of the working face begin to combine with the collapsed roof strata of the adjacent (4-5) 04 goaf, forming an S-shaped overlying strata spatial structure. When the working face is mined to the square position of the two working faces, the rock strata fracture height reaches its maximum but does not reach the key stratum, as shown in Figure 8D. During this stage, the high-located key stratum remains stable, and with the working face continuing to be mined, the range of the fractured rock strata will not increase in both plane and height directions. Therefore, although the mining-induced seismicity events will gradually appear, no high energy level mining-induced seismicity will occur, and the energy and frequency of mining-induced seismicity events will increase less compared to the low-located roof strata movement stage.

(3) Coal pillar-key stratum structure formation stage.

The mining range corresponds to the distance between the working face from the flush position of the original (4–5) 02 open-off cut to the instability position of the remaining coal pillar. The movement characteristics of the rock strata are characterized by the wide remaining coal pillar effectively supporting the key stratum without destabilization and isolating the series movement of the rock strata on both sides of the goaf to form the coal pillar-key stratum structure. After the mining position of the working face exceeds the open-off cut of the original (4-5) 02 working face, due to the blocking effect of the wide remaining coal pillar (40 m), the overlying strata of the (4-5) 02 goaf and the

small structure of the (4-5) 04/06 goaf will not be connected. Therefore, the height and range of rock strata fracture will not increase, and the key stratum keep the overhanging top state, as shown in Figure 8E. During this stage, the wide remaining coal pillar is gradually damaged by the superposition of lateral support pressure on both sides of the goaf, which reduces the bearing capacity of the coal pillar, and the coal pillar-key stratum structure gradually develops from a steady state to an unstable state. Therefore, medium energy level mining-induced seismicity events start to appear, the mining-induced seismicity enters the active period, and the energy and frequency of the mining-induced seismicity increase significantly compared with the overlying strata spatial structure expansion stage.

(4) High-located key stratum movement stage.

The mining range corresponds to the distance between the working face from the instability position of the remaining coal pillar to the square position of the three working faces. The movement characteristics of the rock strata are characterized by the instability of the wide remaining coal pillar which cannot effectively carry the key stratum. The high-located key stratum is unstable after reaching the fracture step of the key stratum, forming a large spatial structure of overlying strata in the three goaves. When the working face is mined to the square position of the third working face, the S-type overlying strata spatial structure is broken periodically to produce a high dynamic load. The wide remaining coal pillar loses its bearing capacity under the superposition of static and dynamic load of lateral support pressure on both sides of the goaf. The fractured rock strata on both sides of the coal pillar are combined, and the overhanging area of the key stratum increases, becoming unstable after reaching the tensile fracture step, as shown in Figure 8F. During this stage, the spatial structure height of the overlying strata reaches its maximum value, that is, the rock layer ruptures into the key stratum. Because the key stratum accumulates very high elastic energy and releases a large amount of elastic energy when it stretches, breaks, and sinks, high energy level mining-induced seismicity events are mainly induced by key stratum fracture. As a result, the mine earthquake in this stage enters a period of frequent occurrence, and the energy level of the mine earthquake is high, and the energy and frequency of mine earthquakes are increased in the mining process. This leads to the frequent occurrence of mining-induced seismicity during this stage, and the energy level of mining-induced seismicity is high, and the energy and frequency of mining-induced seismic events are at a high level in the mining process.

(5) Overlying strata spatial structure periodic movement stage.

The mining range corresponds to the distance between the working face from the square position of the three working faces to the position of the stopping line. The movement characteristics of the rock strata are characterized by periodic breakage of the high-located strata and periodic formation of large structures in the overlying strata space. After the working face is mined past the square position of the three working faces, the plane range and height of the overlying strata fracture will not continue to increase. As the working face continues with mining, the S-shaped space structure that has been formed will fracture periodically. In this stage, the motion state of the key stratum is periodic breaking and rotation, and the energy released in this process is much lower than that released during the initial breaking of the key layer. As a result, the number of mining-induced seismic events will decrease dramatically, and the energy and frequency of mining-induced seismic events will be significantly reduced compared to the previous stage.

4.3 Classification and reliability verification of mining-induced seismicity danger zone

4.3.1 Classification of mining-induced seismicity danger zone and site condition verification

Combining Figures 5–8, we can get the following classification results of the mine earthquake danger zone during the mining of the (4-5) 06 working face of Liuhuanggou Coal Mine.

First of all, according to the 27-2 borehole histogram of the mine, the key stratum is a thick sandstone layer group, with a thickness h of approximately 270 m, and the distance between the key stratum floor and the coal seam is approximately 54 m. Based on the evolution law of spatial structure of overlying strata during the mining of the working face, it can be seen that in the early stage of mining of the (4-5) 06 working face, that is, the low-located roof strata movement stage and overlying strata spatial structure expansion stage, there will be no key stratum fracture type mining-induced seismicity. When the working face is mined to the original (4-5) 02 working face open-off cut, the working face is transformed from a non-seismic dangerous working face to a "mining-induced seismicity working face."

Secondly, since the dip angle of the coal seam is approximately 29°, the stress component Q = 6 MPa is taken as the gravity stress perpendicular to the central line of the key stratum. Considering the weakening effect of the four-edged simple support of the key stratum and the overall strength of the composite key stratum, the allowable tensile strength of the key stratum is R_t = 5 MPa. The Poisson's ratio of the key stratum is μ = 0.25, and the width of the key stratum is the sum of the width of the (4–5) 02/04/06 working face and the width of section coal pillar, then m = 540 m. Substituting the above parameters into Eq. 5, the fracture step of the key stratum is L_{st} = 555.56 m.

Finally, according to the method for predicting the possibility of mining-induced seismicity occurrence in thick and hard key stratum working faces, it is known that the (4-5) 06 working face will be in danger of mining-induced seismicity during the high-located key stratum movement stage. Based on the thick plate theory, the fracture step of the key stratum in the Liuhuanggou coal mine is calculated to be 555 m. Considering the error of the theoretical calculation, the (4-5) 06 working face is drawn to a range of 500–600 m from the original (4-5) 02 open-off cut, where there is a risk of main key stratum fracture-type mining-induced seismicity.

On 10 December 2019, a high energy level mining-induced seismic event with an energy of 5.17 E+07J occurred at the (4-5) 06 working face with a source location that was approximately 512 m from the flush position of the open-off cut at the (4-5) 02 working face. On 19 January 2020, a high energy level mining-

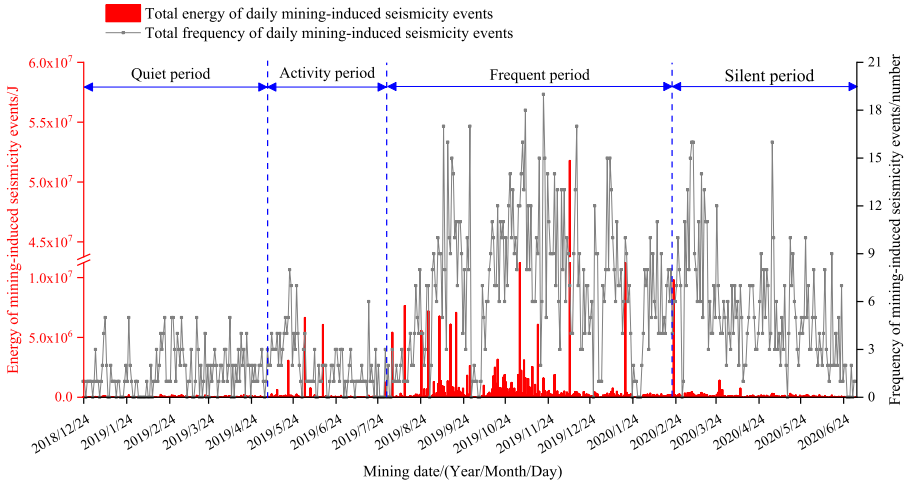

FIGURE 9
Time series characteristics of mining-induced seismicity activity in (4–5)06 working face.

induced seismic event with an energy of 1.7 E+07J occurred in the goaf behind the (4-5) 06 working face with a source location that was approximately 556 m from the flush position of the open-off cut at the (4-5) 02 working face. This shows that the derived fracture step of the key stratum based on the thick plate theory is consistent with the actual occurrence of mining-induced seismicity in the field, and can be used as the theoretical basis for mining-induced seismicity grade prediction.

4.3.2 Verification of time distribution law of key stratum fracture type mining-induced seismicity

The total number of microseismic events of grades < 1.2 in the (4-5) 06 working face accounted for 83.1%. This percentage of microseismic events was mainly generated by the fracture of coal and rock masses and low-located overlying strata movements caused by normal mining at the working face, with the characteristics of high frequency and low energy. Because of the small influence on the analysis of the mining-induced seismicity occurrence law at the working face, only the microseismic events of grades ≥1.2 were selected as the mining-induced seismicity level for analysis.

The time distribution series of mining-induced seismicity reflects the characteristics of overlying strata movement caused by the mining of (4-5) 06 working face. The curve of total energy and total frequency of daily mining-induced seismicity during the period from initial to final mining of the working face is shown in Figure 9. From the figure, it can be seen that the "zonality" of daily mining-induced seismicity energy and frequency with time during mining at the working face is obvious. The curve can be divided into four periods according to the variability of its distribution, while the time series of mining-induced seismicity occurrences correspond to the five stages of spatial structure evolution of overlying strata.

(1) Quiet period of mining-induced seismicity.

In the period from 24 December 2018 to 9 May 2019, the average frequency of mine earthquakes was approximately 1.6 times/d and the average energy was approximately 5.4 E+04J/d, showing the characteristics of low frequency and low energy. During this stage, the working face was mined to 370 m from the open-off cut, and the working face experienced the influence of the overlying strata movement of the square of a single working face but did not reach the two working faces square influence area. The frequency of mining-induced seismicity was in a very low state, mainly due to the fact that the formation range of the overlying strata spatial structure was small, which corresponds to the low-located roof strata movement stage in the spatial structure evolution of overlying strata.

(2) Activity period of mining-induced seismicity.

In the period from 10 May 2019 to 29 July 2019, the average frequency of mining-induced seismicity was approximately 2 times/d, and the average energy is approximately 2.7 E+05J/d. The frequency and energy level of mining-induced seismicity were higher than those in the quiet period, showing the characteristics of low frequency and high energy. During this stage, the working face was mined to 370 m from the open-off cut, which had not yet reached the original (4-5) 02 working face open-off cut flush position. Mining-induced seismicity was mainly concentrated in the period of two working face square, with paroxysmal activity characteristics. It can be seen that with the mining of (4-5) 06 working face, the spatial structure range of overlying strata increased and started to appear gradually, which corresponds to the overlying strata spatial structure expansion stage in the spatial structure evolution of overlying strata.

(3) Frequent periods of mining-induced seismicity

In the period from 30 July 2019 to 23 February 2020, the average frequency of mining-induced seismicity was approximately 6.9 times/d, and the average energy is approximately 1.1 E+06J/d. The frequency and energy level of mining-induced seismicity had a large transition compared with the active period, showing the characteristics of high frequency and high energy. During this

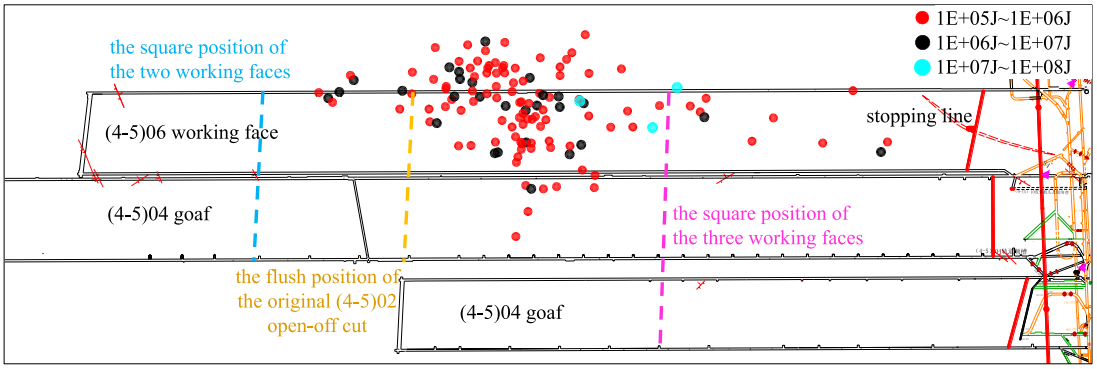

FIGURE 10
Planar projection of high-energy mining-induced seismic events in the (4–5) 06 working face.

stage, the working face was mined to 1,260 m from the open-off cut and experienced the influence of the overlying strata movement of the second square of the two working faces and the square of the three working faces, which led to the frequent occurrence of mining-induced seismicity and the periodic occurrence of large energy mining-induced seismicity (>1 E+05J), and the occurrence of mining-induced seismicity showed zonal concentration. It shows that with the overlying strata movement in series in the three goaves, the spatial structure range of overlying strata reaches the maximum. The fracture and rotation of high-located rock strata release a large amount of elastic energy, which induces many strong mining-induced seismic events. This corresponds to the coal pillar-key stratum structure formation stage and the high-located key stratum movement stage in the spatial structure evolution of overlying strata, in which the maximum level of mining-induced seismicity occurs in the high-located key stratum movement stage.

(4) Silent period of mining-induced seismicity.

In the period from 24 February 2020 to 24 June 2020, the average frequency of mining-induced seismicity was approximately 4.5 times/d, and the average energy was approximately 1.3E+05J/d. The frequency and energy level of mining-induced seismicity appeared to be substantially lower compared with the frequent period, showing the characteristics of high frequency and low energy. During this stage, from the square of three working faces to the end of mining, the frequency of mine seismic occurrences was low and no high energy level mine seismic events occurred in the working face. It can be seen that the spatial structure range of overlying strata was no longer developed, and the energy released by the periodic fracture of rock strata in the structure was small, which corresponds to the overlying strata spatial structure periodic movement stage in the spatial structure evolution of overlying strata.

As shown in Figure 10, from 1 January 2019 to 11 December 2019, a total of 8, 432 mining-induced seismic events were monitored in the (4-5) 06 working face and its surroundings, including 123 mining-induced seismic events with energy exceeding 1 E+05J, accounting for 1.46% of the total number. There were 29 mining-induced seismic events with energy exceeding 1 E+06J, of which 26 occurred after the original open-off cut position of the working face footage level (4-5) 02 working face, accounting for 89.7%. The occurrence of high-energy

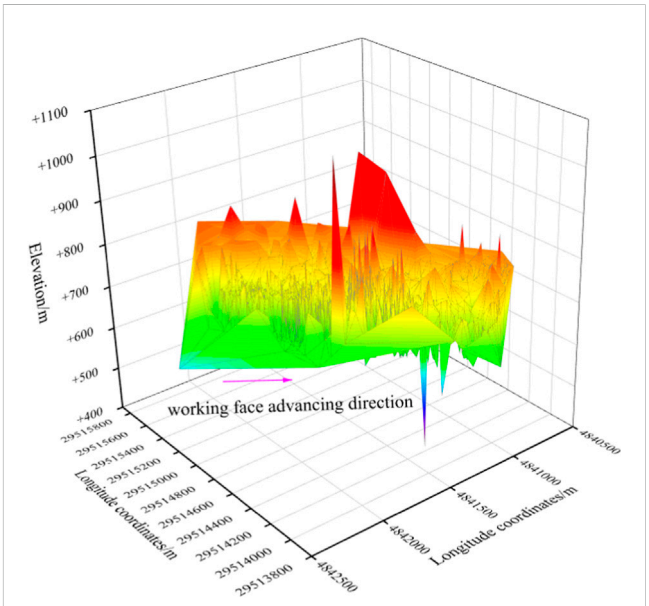

FIGURE 11
Mining-induced seismicity events elevation while mining the (4-5) 06 working face.

mining-induced seismic events was caused by the damage and rupture of high-level rock strata. The high-energy mining-induced seismic events since the mining of the working face were concentrated after the mining position of the working face crossed the open-off cut of the (4-5) 02 working face and the high-energy mining-induced seismicity events were concentrated on the solid coal side of the working face, indicating that the small structure formed by the rock strata in the goaf of the (4-5) 04/06 working face was in motion after the connection with the rock strata in the goaf of the (4-5) 02 working face, and the spatial structure range of the overlying strata was increasing.

4.3.3 Verification of spatial distribution law of key stratum fracture type mining-induced seismicity

The ARAMIS microseismic monitoring system is used to monitor microseismic events in the process of mining in the Liuhuanggou coal mine. Due to an inherent error in the system, the rock fracture layers

cannot be truly represented in the height direction, but the elevation projection of all microseismic events can reflect the changing trend of overlying strata fracture. By projecting the three-dimensional coordinates of all mining-induced seismic events during the mining of (4-5) 06 working face, the variation characteristics of mining-induced seismic events with the mining of the working face can be obtained, as shown in Figure 10.

In the early stage of working face mining, the fracture height of overlying strata was maintained in a certain range. With the advancement of the working face, the fracture height of the roof shows a rising trend, and there was an obvious increase in the fracture height. During the advancement of the working face, the overlying strata kept collapsing, the fracture height of the strata kept rising, and the elevation of the mining-induced seismic events also kept rising, indicating a consistency between the mining-induced seismicity and the fracture of the overlying strata. This indicates that there is consistency between the mining-induced seismicity and the fracture of the overlying strata, that is, the fracture movement of the rock strata induced the mining-induced seismicity.

According to Figure 11, there were three regional high values of the mining-induced seismic event elevation, which were within the influence of the square of the (4-5) 06 working face, the square of the (4-5) 06/04 working faces, and the square of the (4-5) 06/04/02 working faces. The highest value of mining-induced seismic event elevation was located in the influence area of the square of three working faces, and the rock fracture layer was much higher than the square of the two working faces. The fractured rock strata were close to the upper part of the working face during the square of the single working face and two working faces, and the fractured rock strata were distributed in the upper, middle, and lower parts of the working face during the square of the three working faces, indicating that the range of the goaf has a high influence on the fracture height of the rock strata. Before the square of the three working faces, the rock strata rupture mainly occurred in the low rock layer, and the key stratum was in the overhanging top state. When the working face was mined to the square of the three working faces, the mining-induced seismicity elevation increased significantly, the key stratum was broken, the rupture range was large, and the released energy was high, which induced high energy level mining-induced seismicity.

4.4 Verification of the damage to surface buildings induced by mining-induced seismicity

4.4.1 Mining-induced seismic energy estimation

Take the key stratum elastic modulus E=10 GPa, and substitute the remaining parameters of the key stratum into Eq. 7 to obtain the original elastic energy of accumulation in the key stratum U_1=8.54 E + 09 J. According to the 27–2 borehole histogram, it can be seen that there were rock strata with a thickness of approximately 54 m between the 4-5 coal seam and the main key stratum. Because the rock strata have all been broken, take ζ=0.1, the elastic energy accumulated under the action of horizontal stress of low-located key stratum breaking transfer is U_2=6.83 E+07J. According to the observation data of mine surface subsidence, it can be seen that there was no obvious subsidence on the surface after the high energy level mining-induced seismicity. Therefore, it can be determined that a masonry hinged stable structure was formed between the key stratum of the fracture, the elastic energy U_3=0 J generated by the work done by the instantaneous subsidence movement after the breakage of the deflection deformation of the high-located key stratum.

Taking the conversion rate of breaking release energy into vibration energy K=1%, the key stratum breaking release energy U was actually converted to transfer kinetic energy in the form of vibration wave U_K=8.6 E+07J, and the theoretical maximum magnitude of the key stratum breaking is 3.2 according to the magnitude conversion formula (D = (log(U)-1.8)/1.9, D is the level of mining-induced seismicity; U is the monitoring energy of mining-induced seismicity, J). The maximum grade of mine earthquake in the mining process of (4-5) 06 working face of Liuhuanggou Coal Mine was 3.1. The theoretical calculation result is consistent with the actual situation, which verifies the rationality of the prediction of the grade of mining-induced seismicity induced by key stratum fracture based on the thick plate theory.

4.4.2 Assessment results of surface buildings vibration damage induced by high energy level mining-induced seismicity

Taking the energy conversion coefficient between the vibration energy and particle kinetic energy λ = 0.01, rock medium ρ = 26 kN/m^3, vibration wave attenuation coefficient η = 2, the particle vibration velocity v_m = 30 mm/s, and v_m = 5 mm/s, each can be substituted into Eq. 15 respectively to obtain a vibration damage boundary R_1 of approximately 858 m and a vibration perception boundary R_2 of approximately 5,148 m.

The source of the largest energy level mining-induced seismic event in the Liuhuanggou Coal Mine was approximately 1,300 m away from the surface office building and approximately 1,500 m away from the staff apartment, which is beyond the vibration damage boundary, so the mine earthquake was significantly felt in the office building and staff apartment when it occurred, but no significant damage occurred.

4.4.3 Assessment results of surface building vibration damage induced by frequent mining-induced seismicity

The amount of damage to the structural elements of the building is generally 1 E+04. The main frequency of the key stratum fracture type mining-induced seismicity $f \leq$ 10 Hz, thus we took f = 9 Hz. The average wave delay time of the vibration wave is 1s. According to the frequency of high energy level mining-induced seismic events in the (4-5) 06 working face, the average number of mining-induced seismic events per year is n = 55 times. Substituting the above data into Formula 17, it can be obtained that the service life of the building is 20 years when it reaches the critical damage value under the action of frequent mining-induced seismicity.

In summary, it can be seen that the surface buildings of Liuhuanggou Coal Mine will not be damaged under the influence of high energy level mining-induced seismicity, but the service life of the surface buildings is only 20 years under the influence of frequent high energy level mining-induced seismicity. Therefore, it is necessary to study the prevention and control measures of mining-induced seismicity to reduce the energy and frequency of mining-induced seismicity, so as to ensure the long-term safety and stability of the mine surface buildings.

TABLE 2 Table of vibration effects.

Particle vibration Velocity/mm·s^{-1}	Vibration effect
<1	Such nuances are beyond human perceptibility
1	The subtle tremors perceptible to human senses
5	The palpable vibrations engender discomfort, a sense of quaking — notably in earthen kilns, adobe homes, and stone houses where safety from seismic velocities is paramount
10	The conspicuous tremors instigate profound unease and palpable disturbance
30	Provokes an intense sensation of trembling, surpassing the safe seismic velocities of industrial and commercial structures
50	Exceeds the general safety threshold of seismic disturbances for civilian residential structures
100	Surpasses the stringent limits of seismic vibrations set for reinforced concrete structures and tunnel support systems
140	The vibrations instigate the formation of fractures in the rock medium and the amplification of existing fissures
190	The vibrations lead to substantial cracking and devastation within typical civilian edifices
300	The vibrations precipitate the dislodgment of rock within the unsupported tunnel systems
600	The vibrations engender the emergence of novel fissures within the rock structure

5 Discussion

Research has shown that particle vibration velocity is the most commonly used indicator to distinguish personnel's vibration sensation and ground building vibration damage. Different levels of mining-induced seismicity generate different particle vibration velocities when they propagate to the ground. According to the magnitude of particle vibration velocity, the range of ground vibration caused by mining-induced seismicity can be divided as shown in Table 2. The main coal producing areas in China, such as Shandong, Inner Mongolia, Xinjiang, and Heilongjiang, all have extremely thick hard rocks. As the underground mining area increases, the thick and hard key layers break and move during the mining process, resulting in mining-induced seismicity. Production site practice shows that a large number of 2.0–3.0 level mining-induced seismic events occur. Although they do not cause damage to surface buildings, the strong seismic sensation caused by mining-induced seismicity causes panic among a large number of residents on the ground. Mining-induced seismicity has had a great impact on the psychological and mental health of the people, so it has gradually begun to pose a threat to social and public safety. Therefore, conducting reliable prediction of coal mine roof motion induced mining-induced seismicity and induced disasters is a major requirement for safe and efficient coal mining in China.

Unlike other studies, this article proposes a mining-induced seismicity prediction method and hazard assessment method based on the spatial structure evolution characteristics of overlying strata and the motion state of the key stratum in the working face. It can quantitatively calculate the magnitude of mining-induced seismicity energy through different mining stages, and achieve quantitative prediction of mining-induced seismicity and hazard throughout the whole mining cycle of the working face and mine. However, the method proposed in this article is mainly based on typical geological conditions and mining technical conditions. When applied in mines with special geological structures and unconventional mining methods, specific factors need to be considered for improvement and analysis. Therefore, it only provides an engineering reference for mines with similar geological conditions and mining technical conditions. The authors will further optimize the mining-induced seismicity prediction method in future research, taking into account multiple factors such as different geological structures, coal seam thickness, mining methods, coal pillar retention, and geological structures, to achieve quantitative prediction of various types of mining-induced seismicity, thereby ensuring the safety of mine production and the psychological and general health of personnel.

6 Conclusion

In this article, the methods of field investigation, theoretical analysis, and microseismic monitoring were used to propose a prediction method for the possibility of mining-induced seismicity and a risk assessment method for induced disasters in thick and hard key stratum working faces. Taking the (4-5) 06 working face of Liuhuanggou Coal Mine as the engineering background, the on-site microseismic monitoring verification of the overburden structure and the quantitative calculation of the induced disaster risk are carried out. The following research conclusions are drawn in this article:

(1) Based on the evolution law of spatial structure of overlying strata and the movement state of the key stratum, the prediction method of mining-induced seismicity in thick and hard key stratum working faces was proposed. The risk of mining-induced seismicity is mainly related to the boundary conditions of the working face, the thickness of the key stratum, the distance from the coal seam to the key stratum, the height of the overlying strata spatial structure of the working face, and the fracture step of the key stratum.
(2) Based on the thick plate theory, the formula for estimating the ultimate tensile fracture step of the key layer was derived. The estimation method of the fracture-type mining-induced seismicity energy of the key stratum was proposed, which

included the elastic energy of rock accumulation, the elastic energy of rock fracture transfer, and the elastic energy of rock gravitational potential energy conversion. The rationality of the theoretical calculation formula was verified by actual field measurement data.

(3) A ground vibration damage effect model induced by mining-induced seismicity was established based on the "goaf boundary—surface movement boundary—vibration damage boundary." The assessment method for vibration damage of surface buildings induced by high energy level mining-induced seismicity based on particle vibration velocity was proposed, and the vibration damage boundary and vibration perception boundary were calculated. An assessment method for vibration damage of surface buildings induced by frequent low energy level mining-induced seismicity based on building vibration fatigue damage was proposed.

(4) The spatial structure evolution of overlying strata was divided into five stages according to the changes in boundary conditions in the mining process of the (4-5) 06 working face. Based on this, the risk area of mining-induced seismicity in the working face was calculated, and the spatial and temporal distribution law of the mining-induced seismic events in the working face was studied. The "zonality" characteristics of time series and the "transition" law of spatial distribution were obtained, and the reliability of the mining-induced seismicity prediction method was verified.

Data availability statement

The datasets presented in this study can be found in online repositories. The names of the repository/repositories and accession number(s) can be found in the article/Supplementary Material.

Author contributions

All authors listed have made a substantial, direct, and intellectual contribution to the work and approved it for publication.

Funding

This work was supported by the National Key Research and Development Program of China (No. 2022YFC3004604); the Young Talents Lifting Project of China Association for Science and Technology, (No. 2021QNRC001); the Major Science and Technology Innovation Project of Shandong Province, (No. 2019SDZY02); Supported by Shandong Energy Group, (No. SNKJ2022BJ01-R27); the open fund of State Key Laboratory of Coal Mine Disaster Dynamics and Control (2011DA105827-FW202209).

Conflict of interest

Author XZ was employed by the company Shandong Energy Group Co., Ltd.

The remaining authors declare that the research was conducted in the absence of any commercial or financial relationships that could be construed as a potential conflict of interest.

The reviewer ZC declared a shared affiliation with the author TY to the handling editor at time of review.

Publisher's note

All claims expressed in this article are solely those of the authors and do not necessarily represent those of their affiliated organizations, or those of the publisher, the editors and the reviewers. Any product that may be evaluated in this article, or claim that may be made by its manufacturer, is not guaranteed or endorsed by the publisher.

Supplementary material

The Supplementary Material for this article can be found online at: https://www.frontiersin.org/articles/10.3389/feart.2023.1238055/full#supplementary-material

References

Baranov, S. V., Motorin, A. Y., and Shebalin, P. N. (2021). Spatial distribution of triggered earthquakes in the conditions of Mining-Induced seismicity. *Izvestiya, Phys. Solid Earth* 57 (4), 520–528. doi:10.1134/s1069351321040029

Chlebowski, D., and Burtan, Z. (2021). Mining-Induced seismicity during development works in coalbeds in the context of forecasts of geomechanical conditions. *Energies* 14 (20), 6675. doi:10.3390/en14206675

Dou, L., Cao, J., Cao, A., Chai, Y., Bai, J., Kan, J., et al. (2021). Research on types of coal mine tremor and propagation law of shock waves. *Coal Sci. Technol.* 49 (06), 23–31. doi:10.13199/j.cnki.cst.2021.06.003

Grzegorz, M., Adam, L., and Zbigniew, Z. (2020). Prediction of rotational ground motion for mining-induced seismicity – case study from Upper Silesian Coal Basin, Poland. *Eng. Geol.* 276, 105767. doi:10.1016/j.enggeo.2020.105767

Guangyao, S., Wu, C., Shuyu, W., and Xu, L. (2020). Prediction of relatively High-Energy seismic events using spatial–temporal parametrisation of Mining-Induced seismicity. *Rock Mech. Rock Eng.* 53, 5111–5132. doi:10.1007/s00603-020-02210-3

Hou, D., Su, X., Wang, W., Du, F., and Zhao, Y. (2023). Water inrush mechanism in fault fracture zone based on a nonlinear mechanical model of three flow fields. *Geofluids* 2023, 1–9. doi:10.1155/2023/4743053

Jan, D., and Jacek, M. (2018). Mining-induced seismicity of a seam located in rock mass made of thick sandstone layers with very low strength and deformation parameters. *J. Sustain. Min.* 17 (04), 167–174. doi:10.1016/j.jsm.2018.08.002

Jiang, B., Xin, Z., Zhang, X., Deng, Y., Wang, M., Li, S., et al. (2023). Mechanical properties and influence mechanism of confined concrete arches in high-stress tunnels. *Int. J. Min. Sci. Technol.* 33, 829–841. doi:10.1016/j.ijmst.2023.03.008

Jiang, F., Wei, Q., Yao, S., Wang, C., and Qu, X. (2013). Key theory and technical analysis on mine pressure bumping prevention and control. *Coal Sci. Technol.* 41 (06), 6–9. doi:10.13199/j.cst.2013.06.12.jiangfx.008

Jiang, F., and Yang, S. (2003). Spatial fracturing progresses of surrounding rock masses in longwall face monitored by microseismic monitoring techniques. *J. China Coal Soc.* 28 (04), 357–360.

Jiang, Y., Pan, Y., Jiang, F., Dou, L., Ju, Y., Kaifi, J., et al. (2014). Phase I dose escalation study of capecitabine and erlotinib concurrent with radiation in locally advanced pancreatic cancer. *J. China Coal Soc.* 39 (02), 205–210. doi:10.1007/s00280-014-2488-7

Li, G., Zhu, C., He, M., Zuo, J., Gong, F., Xue, Y., et al. (2023). Intelligent method for parameters optimization of cable in soft rock tunnel base on longitudinal wave velocity. *Tunn. Undergr. Space Technol. incorporating Trenchless Technol. Res.* 133, 104905. doi:10.1016/j.tust.2022.104905

Liu, H., and Zhang, X. (2020). Discriminantanalysisofminequaketype and intensitybasedonadeepneuralnetwork. *Int. J. Comput. Integ. M.* 33 (10-11), 1145–1155. doi:10.1080/0951192X.2020.1718770

Liu, G. J., Li, S. L., Mu, Z. L., Chen, W., Song, L. B., Liu, J., et al. (2021). Numerical study on the impact instability characteristics induced by mine earthquake and the support scheme of roadway. *Shock Vib.* 2021, 1–16. doi:10.1155/2021/7697905

Liu, Z., Zhang, R., Sun, X., and Shang, W. (2021). Cause analysis and control measures for roadway bursting caused by mining-induced tremors of hard roof–a case study of the inner Mongolia coalfield, China. *IOP Conf. Ser. Earth Environ. Sci.* 861 (6), 062087. doi:10.1088/1755-1315/861/6/062087

Lu, A., Dou, L., Bai, J., Chai, Y., Zhou, K., Kan, J., et al. (2021). Mechanism of Hard-Roof rock burst control by the Deep-Hole blasting: numerical study based on particle flow. *Shock Vib.* 2021, 1–14. doi:10.1155/2021/9527956

Lurka, A. (2021). Spatio-temporal hierarchical cluster analys is of mining-induced seismicity in coal mines using Ward's minimum variance method. *J. Appl. Geophys.* 184, 104249. doi:10.1016/j.jappgeo.2020.104249

Ma, X., Westman, E., Slaker, B., Thibodeau, D., and Counter, D. (2018). Thebvalueevolutionofmining-inducedseismicity and mainshockoccurrencesathard-rockmines. *Int. J. Rock Mech. Min.* 104, 64–70. doi:10.1016/j.ijrmms.2018.02.003

Ren, F., Zhu, C., He, M., Shang, J., Feng, G., and Bai, J. (2022). Characteristics and precursor of static and dynamic triggered rockburst: insight from multifractal. *Rock Mech. Rock Eng.* 56 (3), 1945–1967. doi:10.1007/s00603-022-03173-3

Rusek, J. (2017). A proposal for an assessment method of the dynamic resistance of concrete slab viaducts subjected to impact loads caused by mining tremors. *J. Civ. Eng. Environ. Archit.* doi:10.7862/rb.2017.43

Ryszard, H., Wojciech, T. W., Artur, G., and Agnieszka, M. (2020). "Identification of the ground movements caused by mining-induced seismicity with the satellite interferometry," in Proceedings of the International Association of Hydrological Sciences, Delft, the Netherlands, April 2020, 382.

Sokoła-Szewioła, V., and Żogała, M. (2019). Forecast and assessment of the effects of the impact of mining tremors, induced by exploitation, on building objects with the use of GIS system. *IOP Conf. Ser. Earth Environ. Sci.* 261 (1), 012048. doi:10.1088/1755-1315/261/1/012048

Wang, K., Hu, P., and Zhou, J. (2021). Study on structural fatigue damage and safe site selection of adjacent buildings under frequent mine earthquake. *J. Saf. Sci. Technol.* 17 (06), 58–64. doi:10.11731/j.issn.1673-193x.2021.06.010

Wang, G., Zhu, S., Jiang, F., Zhang, X., Liu, J., Wang, X., et al. (2022a). Seismic mechanism of coal pillar-key layer structure in fully mecha-nized caving face of inclined thick coal seam. *J. China Coal Soc.* 47(06):2289–2299. doi:10.13225/j.cnki.jccs.2021.1316

Wang, Q., Xu, S., Xin, Z., He, M., Wei, H., and Jiang, B. (2022b). Mechanical properties and field application of constant resistance energy-absorbing anchor cable. *Tunn. Undergr. Space Technol. incorporating Trenchless Technol. Res.* 125, 104526. doi:10.1016/j.tust.2022.104526

Wang, Z., Li, X., and Shang, X. (2019). Distribution characteristics of Mining-Induced seismicity revealed by 3-D Ray-Tracing relocation and the FCM clustering method. *Rock Mech. Rock Eng.* 52 (01), 183–197. doi:10.1007/s00603-018-1585-z

Wu, D., and Ye, X. (1997). A comprehensive review and commendation of blast vibration safety velocity. *Chin. J. Rock Mech. Eng.* (03), 67–74.

Xue, Y., Liu, S., Chai, J., Liu, J., Ranjith, P., Cai, C., et al. (2023a). Effect of water-cooling shock on fracture initiation and morphology of high-temperature granite: application of hydraulic fracturing to enhanced geothermal systems. *Appl. Energy* 337, 120858. doi:10.1016/j.apenergy.2023.120858

Xue, Y., Ranjith, P., Gao, F., Zhang, Z., and WangWang, S. (2023b). Experimental investigations on effects of gas pressure on mechanical behaviors and failure characteristic of coals. *J. Rock Mech. Geotechnical Eng.* 15 (02), 412–428. doi:10.1016/j.jrmge.2022.05.013

Yang, Z., Liu, C., Zhu, H., Xie, F., Dou, L., and Chen, J. (2019). Mechanism of rock burst caused by fracture of key strata during irregular working face mining and its prevention methods. *Int. J. Min. Sci. Technol.* 29 (06), 889–897. doi:10.1016/j.ijmst.2018.07.005

Ye, D., Liu, G., Wang, F., Gao, F., Yang, T., and Zhu, J. (2023). Fractal hydrological-thermal-mechanical analysis of unconventional reservoir: A fracture-matrix structure model for gas extraction. *Int. J. Heat Mass Transf.* 202, 123670. doi:10.1016/j.ijheatmasstransfer.2022.123670

Yin, Q., Wu, J., Zhu, C., He, M., Meng, Q., and Jing, H. (2021). Shear mechanical responses of sandstone exposed to high temperature under constant normal stiffness boundary conditions. *Geomechanics Geophys. Geo-Energy Geo-Resources* 7 (02), 35. doi:10.1007/s40948-021-00234-9

Zhang, M., Jiang, F., Li, K., Wei, Q., Sun, C., and Guo, X. (2018). Lin28b and Sox2 regulate anesthesia-induced neural degeneration in neural stem cell derived neurons. *J. Central South Univ. Sci. Technol.* 49 (01), 167–172. doi:10.1016/j.ejphar.2017.12.031

Zhang, P., Sun, C., Fan, X., Li, S., Wang, L., and Cao, Z. (2023). Temporal and spatial evolution mechanisms of the water-conducting fractured zone of overlying strata in the kongzhuang coal mine. *Geofluids* 2023, 1–13. doi:10.1155/2023/3790998

Zhu, J., Ma, B., Xie, H., Gao, F., Zhou, H., Zhou, C., et al. (2022a). Differences and connections between mining seismicity and coal bursts in coal mines and preliminary study on coal bursts induced by mining seismicity. *J. China Coal Soc.* 47 (09), 3396–3409. doi:10.13225/j.cnki.jccs.2021.1714

Zhu, S., Liu, J., Jiang, F., Shang, X., Sun, X., Zhang, X., et al. (2022b). Classification, prediction, prevention and control of roof movement-type mine earthquakes and induced disasters in China's coal mines. *J. China Coal Soc.* 47 (02), 807–816. doi:10.13225/j.cnki.jccs.XR21.1800

Zhu, S., Wang, B., Jiang, F., Zhang, X., Sun, X., Sun, X., et al. (2021). Study on reasonable width of isolated coal pillar based on rock burst-mine earthquake coordinated control. *Coal Sci. Technol.* 49 (06), 102–110. doi:10.13199/j.cnki.cst.2021.06.012

Zuo, J., Yu, M., Li, C., Sun, Y., Hu, S., and Li, Z. (2021). Analysis of surface cracking and fracture behavior of a single thick main roof based on similar model experiments in western coal mine, China. *Nat. Resour. Res.* 30 (01), 657–680. doi:10.1007/s11053-020-09735-y